ISSN 1027-4510, Journal of Surface Investigation: X-ray, Synchrotron and Neutron Techniques, 2017, Vol. 11, No. 6, pp. 1265–1271. © Pleiades Publishing, Ltd., 2017.
Original Russian Text © N.N. Mikheev, A.S. Kolesnik, 2017, published in Poverkhnost', 2017, No. 12, pp. 54–61.

Universal Function of Informative-Signal Generation for Quantitative Methods of Scanning Electron Microscopy

N. N. Mikheev[a, *] and A. S. Kolesnik[b]

[a] *Laboratory of Space Material Research, Branch of Federal Research Center "Crystallography and Photonics", Russian Academy of Sciences, Kaluga, 248640 Russia*

[b] *Moscow State Technical University, Kaluga Branch, Kaluga, 248001 Russia*

**e-mail: kmikran@spark-mail.ru*

Received February 12, 2017

Abstract—A new universal function $f(x, z)$ describing electron energy losses over depth $\varphi(z)$ and the lateral distribution of electron energy losses $\psi(x)$ in a scanning electron microscope is developed in the context of a multiple electron scattering model at energies of 1–50 keV in condensed matter, where two groups of backscattered primary electrons are taken into account for the first time.

Keywords: multiple electron scattering, transport length of electrons, backscattered primary electrons, lateral distribution of electron-beam-energy losses

DOI: 10.1134/S1027451017050305

INTRODUCTION

Quantitative electron probing techniques for material diagnostics in micro-, opto- and nanoelectronics, such as quantitative X-ray spectral microanalysis (QXRSMA), cathodoluminescence (CL), induced current (IC), or electron backscattering spectroscopy (EBSS), require data on the spatial and energy distribution of the electron beam in a scanning electron microscope (SEM) over a small sample volume. This information is essential in calculating particle-generated informative signals and in estimation of the spatial resolution upon detection of these signals. At present, this is all the more relevant, as electron beams with a diameter of a nanometer become the routine tool for SEM studies, whereas the linear dimensions of individual microrelief details in modern structures reach tens of nanometers.

Simple analytical functions $\varphi(z)$ that describe the depth distribution of energy losses in QXRSMA were derived in [1–3]. As was assumed in a then-used model, all backscattered electrons (BSEs) of a probe are truly backscattered, i.e., they are primary electrons which undergo single scattering at a large angle of $\theta > \pi/2$ and leave a sample after a certain amount of small-angle interactions. Further (in [4]), a contribution to the electron backscattering coefficient η of a beam of truly backscattered primary particles η_1 and those leaving a sample after multiple scattering η_2 was established, and the in-plane lateral distribution function $\psi(x, y)$ of energy losses was proposed.

This work is aimed at plotting a two-dimensional function $f(x, z) = \psi(x)\varphi(z)$ describing the depth and in-plane distributions of energy losses by SEM probe electrons. For the first time, it takes into account two different BSE groups that allow the energy loss distribution of charged particles to be represented in the bulk of the studied sample. The basic function is the first-approximation solution of the transport equation which describes energy losses by charged particles in a substance [5]. The application of this function in quantitative local X-ray spectral microanalysis (QLXRSMA) and for the description of induced current in a short-circuited diode is considered, as well.

BASIC STATEMENTS AND PRELIMINARY RESULTS OF THE APPLICATION OF SIMULATED DISCRETE MULTIPLE FAST-ELECTRON SCATTERING IN A SUBSTANCE

The basic statements of the model describing the transport processes of fast electrons in a substance and their energy dissipation as a result of inelastic scattering are, as follows.

(i) SEM beam electrons upon their motion in a substance experience elastic and inelastic scattering. The averaged effect of these processes on the spatial distribution of primary electrons in the model was described using the transport length L_{tr} of the electron beam as the universal parameter. It characterizes the range of primary electrons which is followed by the complete loss of directional motion in the sample, i.e.,

all directions for primary electrons become equiprobable. The transport length L_{tr} of an electron beam with an energy of E_0 in a substance with the atomic density N_0 is defined through the transport cross section σ_{tr} of electrons by the formula:

$$L_{tr} = 1/(N_0\sigma_{tr}), \quad (1)$$

where $\sigma_{tr} = \int(1-\cos\theta)\,d\sigma$ is the average cross section over all possible directions of collisions θ, and is the transport cross section of primary electron scattering in a substance.

Taking into account the effect of elastic and inelastic scattering channels on the process of interaction between electrons and a substance

$$\sigma_{tr} = \sigma_{tr}^{el} + \sigma_{tr}^{inel},$$

where σ_{tr}^{el} and σ_{tr}^{inel} are the transport lengths of electrons along the elastic and inelastic scattering channels, respectively. The σ_{tr}^{el} and σ_{tr}^{inel} values are calculated using the formulae for the transport cross sections from [5, 6].

(ii) The model assumes the presence of two flows of primary electrons in the sample bulk. The first flow is formed by electrons that have undergone single scattering at a large angle $\theta > \pi/2$ and leave the sample after a certain amount of small-angle interactions. They are truly backscattered electrons with the coefficient η_1. When moving into the interior of the sample, the effect of multiple scattering on the electron distribution over the ranges z in the target is small. As is hereby shown in [7], the distribution itself is well described by the Gaussian function with the maximum at a distance of $z_{ss} = Z^{-1/3}L_{tr}$ from the surface and by the dispersion $\sigma^2 = 0.5z_{ss}^2$. The second flow of particles is formed by electrons which are either absorbed by the target (absorbed electrons) after multiple elastic and inelastic scattering in the sample, or leave the sample (BSEs with a coefficient η_2). The η coefficient for measured experimentally BSEs is the sum of two groups: $\eta = \eta_1 + \eta_2$. In [4], the ratio of BSE contributions of both groups to coefficient η was established to be, as follows:

$$\eta = \eta_1 + \eta_2 = \eta_1 + 0.24\alpha\eta, \quad (2)$$

where the parameter $\alpha = 1 - \exp\{-[R_e/2.8L_{tr}]^{6.67}\}$.

The range of electrons R_e in the expression for the α parameter at the electron energy E_0 is calculated using the formula [3]:

$$R_e = \int_{E_0}^{0} \frac{dE}{dE/dz} = \frac{E_0^2}{8\pi q^4 N_0 Z \ell n\left(\frac{E_0}{C_m}\right)}, \quad (3)$$

where q is the elementary charge, N_0 is the atomic density in the sample, Z is the average atomic number of the latter, $C_m = 790$ eV.

In samples with $Z < 16$ the α parameter is small (≈ 0), thus $\eta_2 = 0$, and $\eta = \eta_1$, and the function $\varphi(z)$ (see [1]) in such targets retains its status as correct description of the depth distribution of energy losses.

(iii) The distribution of electrons experiencing multiple scattering over ranges z in a sample can be described by means of the modified first-approximation function based on the one-dimensional transport equation which was earlier established in [5]:

$$F_1(\Delta E_p, \Delta E) = A_1 \exp\left\{-\frac{b(\Delta E - \Delta E_p)^2}{0.125E_0\Delta E}\right\}, \quad (4)$$

where $\Delta E = E_p - E$; $\Delta E_p = E_0 - E_p$; A_1 is the normalization factor; b is the coefficient taking into consideration different amounts of atomic electrons involved in inelastic scattering ($b = 1$ at $x > L_{tr}$, $b = 4$ at $x \ll L_{tr}$).

As is shown in [5], the $F_1(\Delta E, \Delta E_p)$ function ensures a trivial and reliable approximation for determining the electron distribution with respect to the one-dimensional and steadily increasing variable ΔE. However, its use in the task concerning the description of electrons over the ranges z in a sample for the case of multiple scattering necessitates the following modification of this function. Two factors making the $F_1(\Delta E, \Delta E_p)$ function different from the required $F(z, z_p)$ one were taken into account. First, it is the recurrent movement of a part of primary electrons towards the surface after passing a path equal to the transport length L_{tr}, whereas for charged particles any scattering direction becomes equiprobable. This factor was considered via trivial balancing of the $F_1(z, z_p)$ function relative to the z_p coordinate, as the recurrent movement of a part of electrons from the beam towards the surface shifts the distribution maximum from $z_p \approx L_{tr}$ to $z_p = 0.77L_{tr}$ and additionally increases electron spread over ranges in the near-surface area. The second factor is the presence of two channels of interaction between primary electrons and the substance: elastic and inelastic scattering. In samples with the average atomic number $Z \geq 28$ elastic scattering dominates upon the formation of the electron path distribution during multiple scattering. The transport length L_{tr}^{inel} along the inelastic-scattering channel thus exceeds L_{tr}^{el} along the elastic scattering channel. For example, in $_{32}$Ge the $L_{tr}^{inel}/L_{tr}^{el}$ ratio is ≈ 10.0 at an electron energy of 20 keV. Therefore, the path distribution function in the sample at $z > z_p$ is identical to $F_1(z, z_p)$. For samples with low Z values it is essential to consider the effect of the inelastic-scattering channel on the electron path distribution. For example, in aluminum ($_{13}$Al) for electrons with an energy of 20 keV the $L_{tr}^{inel}/L_{tr}^{el}$ parameter is ≈ 3.8, in carbon ($_6$C)

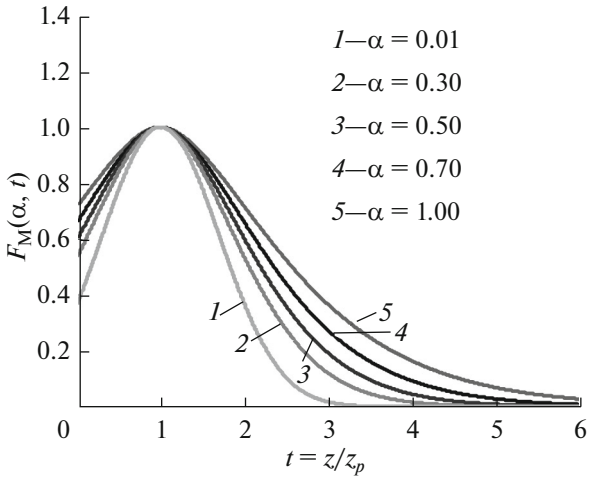

Fig. 1. Modified function of the first-approximation solution of the transport equation for an electron beam that has experienced multiple scattering at α parameter values of 0.01 (*1*), 0.30 (*2*), 0.50 (*3*), 0.70 (*4*), and 1.00 (*5*).

$L_{tr}^{inel}/L_{tr}^{el} \approx 1.6$, and in beryllium ($_4$Be) the $L_{tr}^{inel}/L_{tr}^{el}$ ratio is ≈ 1.15. The effect of this factor on the distribution is thus a weaker particle-range spread dependence on the range value, which is taken into account by introduction of the above parameter α [1].

As a result, the sought one-dimensional electron distribution function over the given ranges (variable $t = z/z_p$) can be obtained from the $F_1(t)$ function by its transformation into the piecewise continuous function $F_M(\alpha, t)$, as follows:

$$F_1(t) \to F_M(\alpha, t) = \begin{cases} \exp\left\{-\dfrac{(t-1)^2}{(\alpha t+1)}\right\}, \text{ at } t \geq 1 \\ \exp\left\{-\dfrac{(t-1)^2}{(1+2\alpha-\alpha t)}\right\}, \text{ at } t < 1 \end{cases}. \quad (5)$$

Figure 1 displays the $F_M(t, \alpha)$ functions plotted for different values of the α parameter. It is seen that varying α from 0.01 to 1.0 causes drastic changes in the distribution at $t > 1$ from a quasi-Gaussian profile to the $F_1(t)$ curve, which is characterized by a quasi-exponential decline in the "tail" range. Modification makes the $F_M(\alpha, t)$ function multipurpose, i.e., the latter becomes suitable for description of the electron distribution over variable t in samples with any Z value.

(iv) It is assumed that samples, subjected to electron bombardment and SEM probing, retain one-to-one correspondence between spatially distributed energy losses of the electron beam and primary electrons distributed over the ranges.

Φ(*Z*) FUNCTION OF INFORMATIVE-SIGNAL GENERATION FOR ELECTRON PROBING TECHNIQUES DESCRIBING THE DEPTH DISTRIBUTION OF ENERGY LOSSES OF AN ELECTRON BEAM

If the transport processes of primary electrons in the sample are considered as the motion of two flows of particles described statistically by multiple and single scattering, respectively, the required function φ(*z*) can be written as the sum of two distribution terms:

$$\varphi(z) = \begin{cases} \dfrac{A_N C_N (1-\eta_1) E_0}{\pi^{1/2} z_p} \exp\left\{-\dfrac{(z-z_p)^2}{z_p[z_p+\alpha(2z_p-z)]}\right\} + \dfrac{1.085\eta_1 Z^{-1/3} E_0}{\pi^{1/2} z_{ss}} \exp\left\{-\dfrac{(z-z_{ss})^2}{z_{ss}^2}\right\}, & z \leq z_p \\ \dfrac{A_N C_N (1-\eta_1) E_0}{\pi^{1/2} z_p} \exp\left\{-\dfrac{(z-z_p)^2}{z_p(z_p+\alpha z)}\right\} + \dfrac{1.085\eta_1 Z^{-1/3} E_0}{\pi^{1/2} z_{ss}} \exp\left\{-\dfrac{(z-z_{ss})^2}{z_{ss}^2}\right\}, & z \geq z_p. \end{cases} \quad (6)$$

where z_p is the depth of maximum energy losses by electrons that have undergone multiple scattering in a sample ($z_p = 0.77 L_{tr}$); z_{ss} is the depth of maximum energy losses by truly backscattered electrons in a sample ($z_{ss} = Z^{-1/3} L_{tr}$); η_1 is the coefficient of truly backscattered electrons; A_N and C_N are the normalization factors. The first term is the distribution of energy losses by electrons that have experienced multiple scattering in a sample, and the second one is the distribution of energy losses by truly backscattered electrons which leave the sample after single scattering at a large angle and a certain amount of small-angle interactions. The A_N coefficient allows one to distinguish the normalization of the function (5) from the Gaussian function at $\alpha > 0$ and is shown in Fig. 2 as function of the α parameter. The C_N coefficient takes into consideration a relative increase in the contribution to the distributed energy losses of absorbed electrons on account of the second BSE group after replacing η by η_1. Its value was found using the following property of the φ(*z*) function: the improper integral of φ(*z*) with respect to *z* in the generation range for a sample with a low mean value of *Z* at $\eta_1 = \eta$ equals the absorbed energy E_{abs} of the electron beam in the studied sample:

$$\int_0^\infty \varphi(z)\, d(z) = E_0\left\{1 - \left[\eta\left(1 - Z^{-1/3}\right)\right]\right\} = E_{abs}, \quad (7)$$

This is due to the fact that the cofactor $(1 - Z^{-1/3})$ in Eq. (7) well describes the average reduced energy

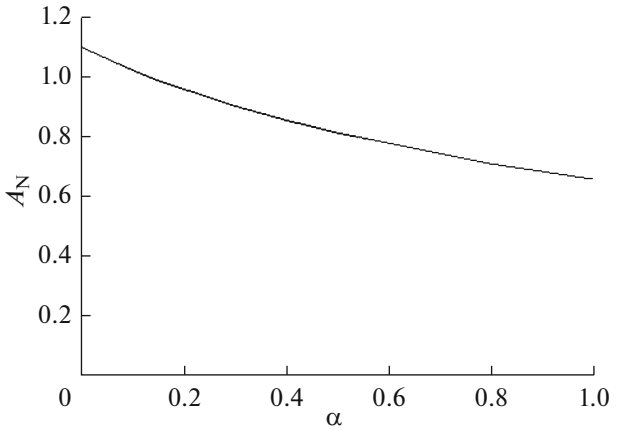

Fig. 2. Normalization factor A_N as a function of the parameter α.

$\langle E\rangle/E_0$ as a function of the atomic number Z of a target for a primary electron beam that experienced single scattering at a large angle and left the sample as a result of backscattering. For materials with any Z value this physically natural property must be preserved by the appropriate choice of the C_N coefficient as:

$$C_N(Z) = \frac{1-\eta+\eta_2 Z^{-1/3}}{1-\eta_1}.$$

The second-term φ(z) function in expression (6), changed relative to φ(z) from [1] due to only truly backscattered electrons being taken into account, and the C_N coefficient arisen in the first term are plotted in Fig. 3 for electrons with an energy of 20 keV in copper and gold samples. The dotted lines denote separately the contributions from each of the two electron flows. It is evident that taking into account two groups of primary electrons in BSE significantly reduces their energy losses in the vicinity of the distribution maxima compared to the approach assuming all BSEs to be truly backscattered.

The compliance of the obtained φ(z) distribution with the experimental spectra of energy losses by electrons of the probe over the target depth of was verified by comparison of the calculated data with the experimental results from classical works [8–10], where the energy loss spectra were established from experiments on thin film perforation (V.E. Cosslett and P.N. Thomas) and by the "labeled layer" method (R. Casteaing, J. Descamps; A. Vignes, and G. Dez). The approved results are displayed in Figs. 4–6. It is obvious that the φ(z) function calculated using formula (6) coincides with the known experimental data over the whole range of the chosen materials (from aluminum to gold) and electron-beam energies (from 10 to 29 keV). This also applies to the distribution-maximum positions, the full width at half maximum (FWHM), and the spectral behavior in the "tail" range of distributions in samples with various atomic numbers Z.

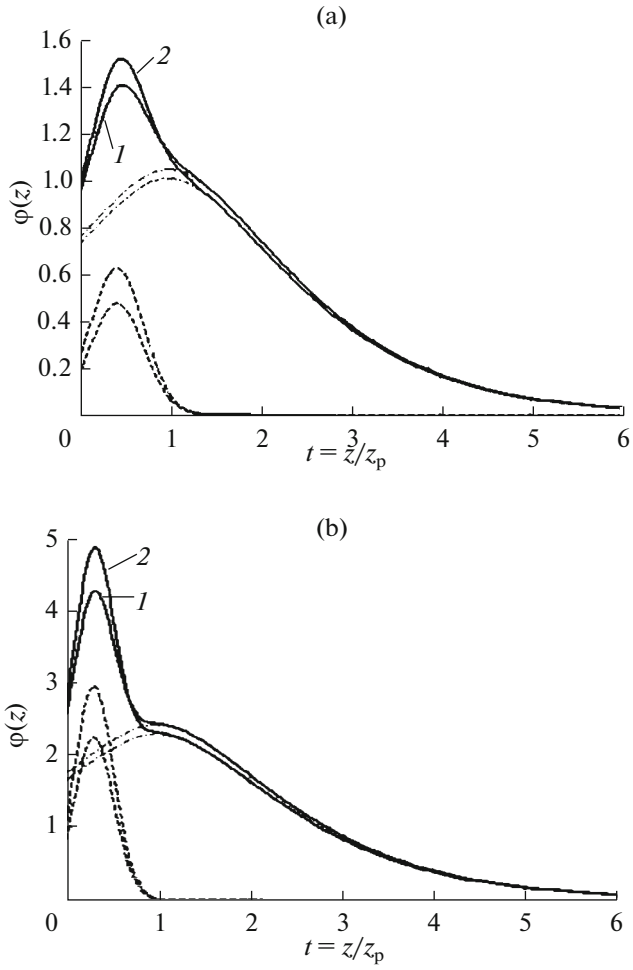

Fig. 3. Depth distribution of electron energy losses at an energy of 20 keV for (a) copper and (b) gold samples: (*1*) taking into account the presence of two groups of backscattered electrons, (*2*) without them taken into account.

From the point of view of practical importance, using φ(z) in the form of φ(ρz) is essential for such a widespread and frequently applied electron probe method as QXRSMA. The most significant matrix correction in X-ray spectral microanalysis is absorption adjustment f_{abs} of the analyzed X-ray line:

$$f_{abs}(\chi) = \int_0^\infty \varphi(\rho z)\exp(-\chi\rho z)d(\rho z) \Big/ \int_0^\infty \varphi(\rho z)d(\rho z),$$

where ρ is the sample density; $\chi = (\mu/\rho)\operatorname{cosec}\theta$, (μ/ρ) is the weight absorption coefficient; θ is the angle of selection of radiation going beyond the sample.

It is evident that a more perfect function φ(ρz) is able to provide higher-accuracy quantitative analysis results in the case of establishment of the real element concentration in the sample. To date, the accuracy required for standard QXRSMA is 2–5%. The application of a new φ(ρz) function for calculation of f_{abs}

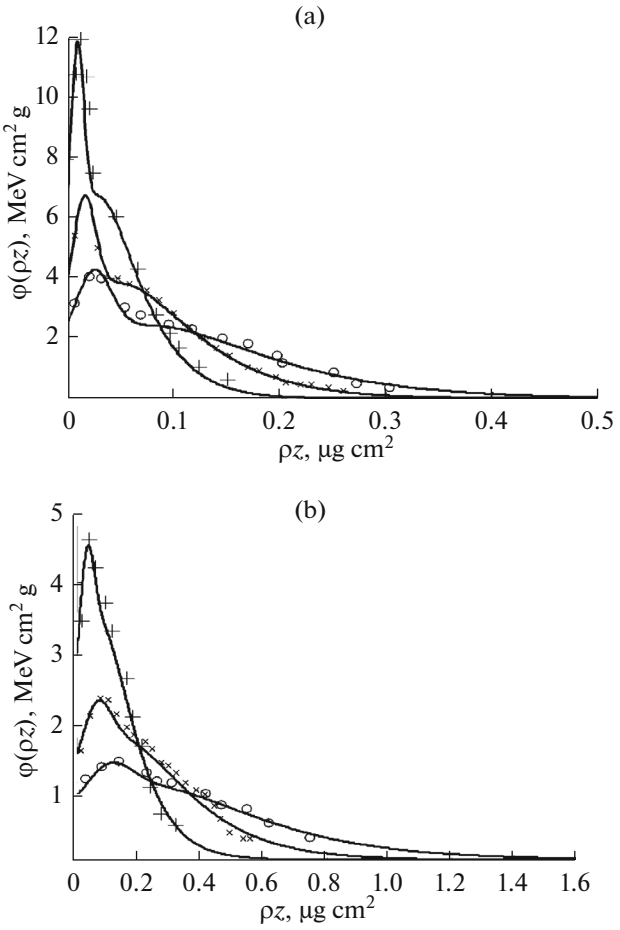

Fig. 4. Results of verification of the obtained energy loss distributions φ(ρz) for the electron beam at energies of 10, 15 and 20 keV (a) in copper and (b) in gold: the solid line shows calculations using Eq. (6); +, × and ○ denote experimental data from [8] for 10, 15 and 20 keV.

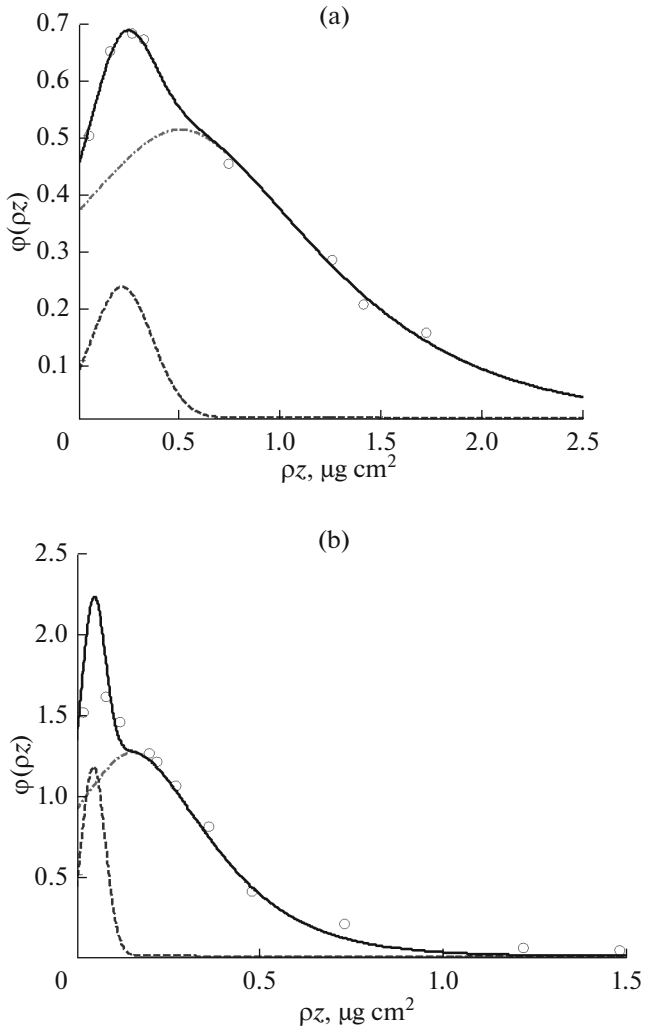

Fig. 5. Results of verification of the obtained energy loss distributions φ(ρz) for the electron beam (a) in copper and (b) in gold at $E_0 = 29$ keV: the solid line shows calculations using Eq. (6) with $\alpha = 1.0$; ○ denotes experimental data from [9], obtained by the labeled layer method.

adjustment in the microanalysis of copper–gold alloys of known composition, as well as comparison of the results with data obtained in [11], reveals that the changes caused by the contribution of two BSE groups and by the replacement of η with η_1 in (6) are small, but they improve the QXRSMA accuracy for the alloy (by 0.1–1.0%).

Ψ(*X*) FUNCTION OF INFORMATIVE SIGNALS FOR ELECTRON PROBING METHODS DESCRIBING THE LATERAL ENERGY LOSS DISTRIBUTION OF AN ELECTRON BEAM

The function ψ(*x*, *y*) describing the in-plane lateral distribution of energy losses was reported in [4]. In the present study, the functional dependence of the energy-loss distribution for truly BSE upon their movement towards the surface was established. It follows that for a small-diameter electron beam ($d \to 0$), incident perpendicularly to the surface of the sample studied, the one-dimensional distribution of energy loss by electrons ψ(*x*) can be written as:

$$\psi(x) = E_0 \left\{ \frac{C_N (1-\eta_1) B_{N1}}{\pi^{1/2} x_p} \exp\left[-\frac{x^2}{x_p (x_p + \alpha x)} \right] + \frac{\eta_1 Z^{-1/3} B_{N2}}{\pi^{1/2} x_{ss}} \exp\left[-\frac{x^2}{0.75 x_{ss} (x_{ss} + x)} \right] \right\}, \quad (8)$$

where: $x_{ss} = 0.275 Z^{-1/3} L_{tr}$, $B_{N1} = 0.92165 A_N$, $B_{N2} = 0.78$.

Here, the first term is the distributed energy losses by absorbed electrons and BSEs thaat have undergone only multiple scattering in the sample. The second term is the distribution of energy losses by truly backscattered electrons which leave the sample after single scattering at a large angle $\theta > \pi/2$ and subsequent multiple small-angle interactions. For this group of BSEs

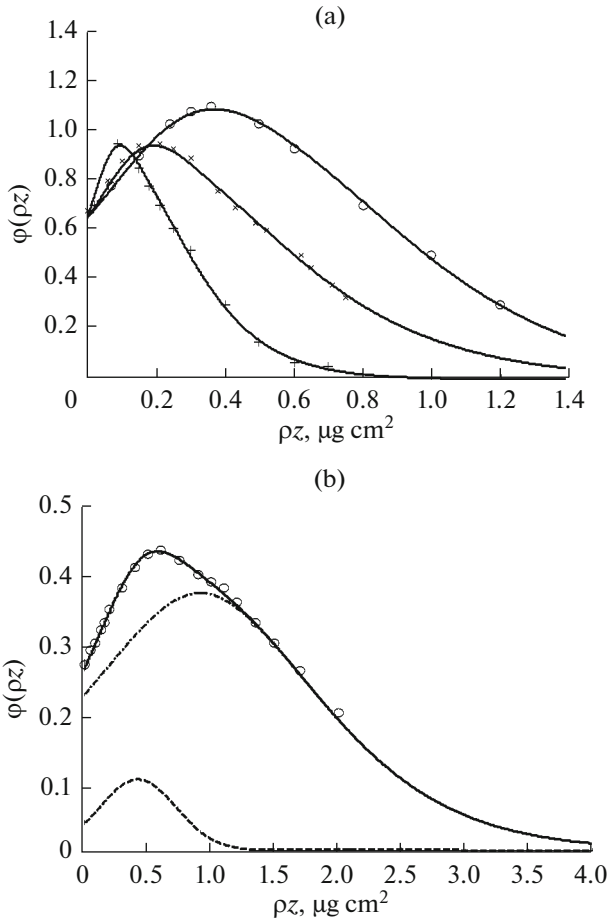

Fig. 6. Results of verification of the obtained energy loss distributions φ(ρz) for the electron beam (a) in aluminum at E_0 = 10, 15, 20 keV: the solid line shows calculations with α = 0.044; o denotes experimental data from [9], obtained by the labeled layer method; (b) in titanium at E_0 = 25 keV; the solid line shows calculations with α = 0.35; the points denote experimental data from [10], obtained by the "labeled layer" method.

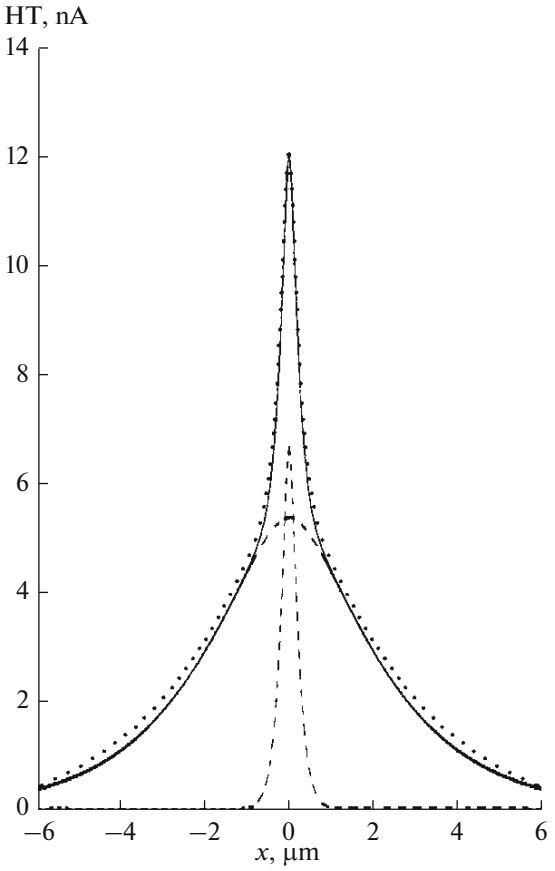

Fig. 7. IC-signal distribution within the cleavage of $GaP_{0.65}As_{0.35}$—*p*–*n*-junction structure—at E_0= 40 keV and $L_{p,n}$ = 0.08 μm: the solid line shows data calculated using Eq. (8); the points show experimental results from [13].

the approximating distribution is a function of the energy-loss distribution over the variable *x* applied to small-angle electron scattering conditions from [12].

When performing SEM studies, one always attempts to implement conditions for the formation of an electron beam with the minimally possible diameter *d* to achieve the best lateral resolution. In modern SEM systems this corresponds to a value of $d \approx 1$–10 nm. In order to take into account the effect of these finite electron-beam sizes on the distribution (8), it is necessary and sufficient to replace the magnitude x_{ss} in ψ(*x*) with $x_{ds} = (x_{ss}^2 + 0.48d^2)^{1/2}$, and x_p by $x_{dp} = (x_{ss}^2 + 0.36d^2)^{1/2}$. Since $x_{ss} \approx 0.1x_p$, the distribution (8) has first to be broadened for truly BSEs due to the finite sizes of the electron beam.

Unlike the φ(*z*) distribution, a direct verification of the ψ(*x*) function is difficult because of a lack of experimental data. However, the validity of the proposed function can be assessed indirectly, using function (8) for calculating the informative signal, such as indirect current in a short-circuited diode, and comparing the calculated IC distribution with the experimentally measured distribution of the same signal. Herewith, the main requirement lies in excluding or minimizing the broadening effect of the narrow peak of energy losses for truly BSEs due to diffusion and drift processes in the electric barrier field of generated non-equilibrium carriers (NECs). These requirements are met for an IC signal detected in a short-circuited diode and upon scanning of a cleavage with an electron probe, perpendicular to the plane of the *p*–*n* junction, of a semiconductor structure with a small diffusion length of NECs and at relatively high energies E_0 of electrons.

As the model experiment for verifying the validity of Eq. (8), we used experimental data from [13], among them were the IC-signal distribution for a cleavage of $GaP_{0.65}As_{0.35}$ (a structure with a *p*–*n* junction) at an electron-beam energy of E_0 = 40 keV and

the diffusion lengths of NECs $L_{p,n} \approx 0.08$ μm. The transport length of electrons with an energy of 40 keV in this material is 2.3 μm at $x_p = 1.77$ μm and $x_{ss} = 0.21$ μm. The IC-signal distribution found from Eq. (8) for describing the lateral distribution of NECs generated by the electron probe is shown in Fig. 7 with a solid line. The contributions of electron–hole pairs associated with the energy losses of two groups of BSEs to the IC signal are depicted with dotted lines, and the points denote the experimentally measured IC signal. Good agreement between the calculated and experimental data is evident, which is on account of the presence of two BSEs groups in the context of the model used.

To conclude, we mention that namely BSEs of the first group, being the main reason for the formation of the narrow peak of energy losses by electrons in a substance, are able to ensure the high spatial locality of studies upon the use of quantitative electron probing methods. It is obvious that its implementation necessitates the application of very thin electron beams with $d \approx 1$ nm at relatively low electron probe energies $E_0 =$ 1–10 keV in research equipment. Thus, high lateral resolution in surface experiments can be achieved in scanning electron microscopes with field or autoemission cathodes.

CONCLUSIONS

A two-dimensional function allowing a trivial analytical description of the spatial distribution of energy losses by an electron beam over depth $\varphi(z)$ and the in-plane lateral distribution $\psi(x)$ in the context of multiple scattering was found.

The validity of the obtained distributions was verified by the comparison of simulation results with experimental data from classical works in a wide range of elements and energies of primary electrons. The dependences calculated using the above function were established to coincide with the experimental ones. Examples of successful application of the function in QXRSMA and for description of the IC signal were shown, also.

ACKNOWLEDGMENTS

This work was partially supported by the Russian Federation for Basic Research and the Government of Kaluga oblast in the framework of the research project no. 14-42-03062.

REFERENCES

1. N. N. Mikheev, M. A. Stepovich, and E. V. Shirokova, Bull. Russ. Acad. Sci.: Phys. **74** (7), 1002 (2010).
2. N. N. Mikheev, M. A. Stepovich, and E. V. Shirokova, Bull. Russ. Acad. Sci.: Phys. **76** (9), 974 (2012).
3. N. N. Mikheev, M. A. Stepovich, and E. V. Shirokova, J. Surf. Invest.: X-ray, Synchrotron Neutron Tech. **7** (6), 1194 (2013).
4. N. N. Mikheev, N. A. Nikiforova, and A. S. Ganchev, J. Surf. Invest.: X-ray, Synchrotron Neutron Tech. **9** (5), 923 (2015).
5. N. N. Mikheev, M. A. Stepovich, and S. N. Yudina, J. Surf. Invest.: X-ray, Synchrotron Neutron Tech. **3** (2), 218 (2009).
6. I. S. Tilinin, Zh. Eksp. Teor. Fiz. **94** (8), 96 (1988).
7. N. N. Mikheev, V. I. Petrov, and M. A. Stepovich, Izv. Ross. Akad. Nauk, Ser. Fiz. **59** (2), 144 (1995).
8. V. E. Cosslett and P. N. Thomas, Br. J. Appl. Phys. D **16** (6), 779 (1965).
9. R. Casteaing and J. Descamps, J. Phys. Radium **16**, 304 (1955).
10. A. Vignes and G. Dez, J. Phys. D: Appl. Phys. **1**, 1309 (1968).
11. N. N. Mikheev, J. Surf. Invest.: X-ray, Synchrotron Neutron Tech. **8** (5), 916 (2014).
12. N. N. Mikheev, Poverkhnost, No. 10, 37 (1998).
13. Q. Oelgart and U. Werner, Phys. Status Solidi A **85** (1), 205 (1984).

Translated by O. Maslova